SIMULATION OF FREE SURFACE FLOW OVER TRAPEZOIDAL OBSTACLE WITH LATTICE BOLTZMANN METHOD

Emrah Korkmaz and Rho-Taek Jung*
School of Naval Architecture and Ocean Engineering, University of Ulsan, Ulsan, Korea

격자볼츠만법을 이용한 장애물 월반 자유수면 시뮬레이션

코르크마츠 엠라, 정 노 택*
울산대학교 조선해양공학부

An air-water free surface flow simulation by using the Lattice Boltzmann Method(LBM) has not been studied a lot compared with the done by the Navier-Stoke equation. This paper shows the LBM is as one of the application tools for the free surface movement over an obstacle. The Mezo scaled application tool has been developed with two dimensional and nine discretized velocity direction using conventional lattice Bhatnagar-Gross-Krook model. Boundary conditions of a halfway-based for solid wall and a kinematic-based for interface are adopted. A validation case with a trapezoidal shape bump to make a comparison between freesurface movements from computational results and experimental ones was described with grid size dependency.

Key Words : Lattice Boltzmann Method, Algorithm of Inclined wall, Dam break

1. Introduction

Since its introduction in 1988[1], the lattice-Boltzmann method(LBM) has become one of the leading methods for computational fluid dynamics. In conventional fluid dynamics methods(CFD), nonlinear partial differential equations that characterize fluid flows solved on discrete elements, nodes, or volumes. In contrast, LBM uses fractious particles that stream along the given direction and collide at lattice point to characterize fluid flows. Having both a particle based structure and simplicity of formulation yields LBM crucial advantages, such as easy to implementation, adaptability on parallel processing systems[2] and handling with complex geometries.

In the computational domain, the particles placing at the grid nodes may be defined with distribution function that denotes probability of collection of particles at a given position, direction, and time. Hence, the distribution function acts as a representative for collection of particles. Using with the distribution function, macroscopic quantities, such as density, velocity, temperature and pressure, are able to obtain for each node.

Defining boundary conditions with regard to the problem has significant effect on LB simulations. Normal bounce-back conditions can be interpreted as either free-slip or non-slip boundary conditions[3]. Depending on the boundary description, either distribution reconstruction or distribution modification can be chosen. With distribution modification, the unknown distribution functions are obtained by some physical rules such as bounce-back rule, mass and momentum conservation law or their combination. In the case of curved boundaries, distribution modification approach need to be interpolated or extrapolated[4,5].

Inclined and complex boundary treatments have to be investigated significantly, especially when real life applications are subjected. To illustrate, free surface motion around offshore substructures is one of the hottest issues in ocean engineering. For this study, we expect to find impact of water to the jacket substructure of offshore

Received: March 3, 2014, Revised: May 29, 2014, Accepted: May 29, 2014.
* Corresponding author, E-mail: rtjung@ulsan.ac.kr
DOI http://dx.doi.org/10.6112/kscfe.2014.19.2.079

wind turbines. A jacket type of substructure consists of many inclined supporting structures.

In this paper, using with the interpolation method for curved boundary conditions, generalized algorithm of inclined wall treatment that helps to get various results for different angles will be presented. The free surface pattern over a trapezoidal obstacle has been observed during two seconds, and the evolution of free surface level at three different locations has been calculated. Furthermore, computational results that have been obtained from scaled computational domain of dam break over an obstacle application were compared with experimental data[6].

2. Lattice Boltzmann Method

The Boltzmann equation modifying with the single relaxation time, named as Bhatnagar Gross Krook (BGK) model[7].

$$\frac{\partial f}{\partial t}+\xi \cdot \nabla f=-\frac{1}{\lambda}(f-f^{eq}) \tag{1}$$

where ξ defines particle velocity, λ defines relaxation time and f^{eq} defines the equilibrium distribution function.

In order to solve f numerically, Eq. (1) needs to be discretized in the velocity space by using a finite set of velocity vectors e_i[8].

$$\frac{\partial f_i}{\partial t}+e_i \cdot \nabla f_i=-\frac{1}{\lambda}(f_i-f_i^{eq}) \tag{2}$$

The nine-velocity square lattice model, which is often referred to as the D2Q9 (2 dimension 9 discrete velocity) model (Fig. 1), has been widely used for simulating two-dimensional flows. In the D2Q9 model:

$$\begin{aligned} e_{i=0} &= (0,0) \\ e_{i=1\sim 4} &= (\cos[(i-1)\pi/2], \\ &\quad \sin[(i-1)\pi/2) \\ e_{i=5\sim 8} &= (\cos[(2i-9)\pi/4], \\ &\quad \sin[(2i-9)\pi/4)\sqrt{2} \end{aligned} \tag{3}$$

denotes the discretized velocity vectors. The equilibrium distribution function for incompressible D2Q9 model is given below[9]

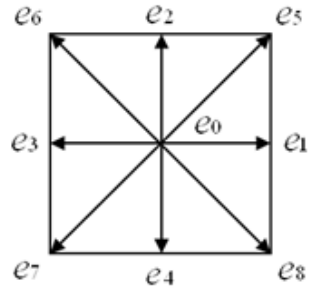

Fig. 1 Discrete velocities of the D2Q9 model

$$f^{eq}=w_i\left[\rho+\frac{3}{c^2}e_i \cdot \boldsymbol{u}+\frac{9}{2c^4}(e_i \cdot \boldsymbol{u})^2 - \frac{3}{2c^2}\boldsymbol{u} \cdot \boldsymbol{u}\right] \tag{4}$$

The weighting factor given by

$$\begin{aligned} w_0 &= 4/9 && \text{i=0} \\ w_i &= 1/9 && \text{i=1-4} \\ w_i &= 1/36 && \text{i=5-8} \end{aligned} \tag{5}$$

In these expressions, the flow properties are defined as:

$$\text{Flow density}: \quad \rho=\sum_{i=0}^{8} f_i \tag{6a}$$

$$\text{Momentum}: \quad \rho u=\sum_{i=0}^{8} f_i e_i \tag{6b}$$

Discretizing Eq. (2) with the time step δ_t[s] and the size of a LBM cell δ_x[m] gives the lattice Boltzmann equation,

$$\begin{aligned} &f_i(x+e_i\delta t, t+\delta t)-f_i(x,t) \\ &\quad =-\frac{1}{\tau}\left[f_i(x,t)-f^{eq}(x,t)\right] \end{aligned} \tag{7}$$

where $\tau=\lambda/\delta_t$, and x is a point in the discretized physical space.

3. Boundary Conditions

3.1 Boundary condition for straight wall

Implementing the bounce-back condition is very simple,

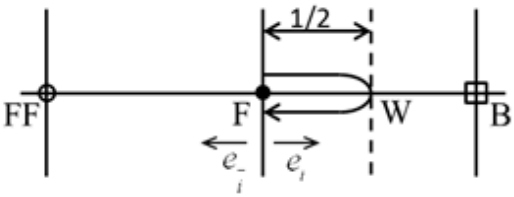

Fig. 2 Wall position at the end of fluid domain

easy and efficient. In the standard bounce-back scheme (bounce-back at nodes), the wall placed at the lattice nodes, i.e. Δ=1 referred as a fraction of an intersected link in the fluid domain in Fig. 2.

$$\Delta = |FW| / |FB| \tag{8}$$

First order accuracy is provided by standard scheme, to obtain a second order accuracy in the bounce-back scheme, an improvement called halfway bounce-back (Δ =1/2) condition required[10,11]. Halfway bounce-back condition formulated as:

$$f_{\bar{i}}(x, t+\delta t) = \tilde{f}_i(x,t) \tag{9}$$

where $\tilde{f}_i(x,t)$ denotes after collision step, and $\bar{i}$ denotes opposite direction of I.

3.2 Boundary condition for inclined or curved wall

More realistic geometries i.e. curved or inclined geometries require high order accuracy. The difficulty for curved boundary, compared to that in straight boundary, are not only the boundary is not exactly located on the lattice point or in the middle but also the density or velocity cannot be obtained by conservation law like for the straight boundary. One of the interpolation methods[4] is used to get the unknown distribution functions coming from the curved boundaries. The philosophy behind this method is to apply bounce-back scheme plus the linear or quadratic interpolation for distribution function. In the proposed method, equations obtained by linear interpolation:

$$f_{\bar{i}}(x_f, t+\delta t) = \frac{1}{2\Delta}\tilde{f}_i(x_f,t) + \frac{2\Delta-1}{2\Delta}\tilde{f}_{\bar{i}}(x_f,t) \quad \text{for } \Delta \geq 1/2 \tag{10a}$$

$$f_{\bar{i}}(x_f, t+\delta t) = 2\Delta\tilde{f}_i(x_f,t) + (1-2\Delta)\tilde{f}_{\bar{i}}(x_{ff},t) \quad \text{for } \Delta < 1/2 \tag{10b}$$

3.3 Free surface boundary condition

Interface cells are identified as a transition point between fluid to gas phase. In our numerical study, gas phase is omitted. Therefore, the treatment has to be presented to find out the boundary condition of interface cells, and to construct the missing distribution functions. This missing part can be accomplished by using atmospheric pressure of $\rho_A = 1$. The atmospheric pressure exerts a certain force on the free surface and this force is equated by an opposite force coming from liquid side.

The missing distribution functions can be constructed for each local lattice directions. Assume that position x is an interface cell and position $x + e_i\delta t$ is a gas cell, then the missing distribution function can be found through this equation[12]:

$$f_{\bar{i}}(x, t+\delta t) = f_i^{eq}(u, \rho_A) + f_{\bar{i}}^{eq}(u, \rho_A) - f_i(x,t) \tag{11}$$

3.4 Algorithm of inclined wall

Prior to presenting the results of inclined wall treatment under free surface, the generalized algorithm must be clarified as shown in the following steps.

1. Determine the closest particle distribution function to boundary node for all discrete directions.

(a) Flag initialization for all nodes via defining new array bb; inside the obstacle for every discrete direction bb=1, outside the obstacle for every discrete direction bb=0.

(b) If (bb+fn) ≠ fn, it means fluid particles encounters obstacle.

2. If the fluid particle encounters the boundary node at next time step, calculate the values between boundary node and fluid node for each direction.

(a) According to discrete direction of particle, values have to be calculated via different formulation that derived from simple triangle geometrical rules.

(b) Related with derivation process, depending on Fig. 3 a couple of constant value has to be calculated such as,

$$a = (j-0.5) - m(i - iobs) \tag{12}$$

where $m = \sin\beta_1 / \cos\beta_1$

$$b = \sin\beta_2 / \sin 135^\circ - \beta_2 \tag{13}$$

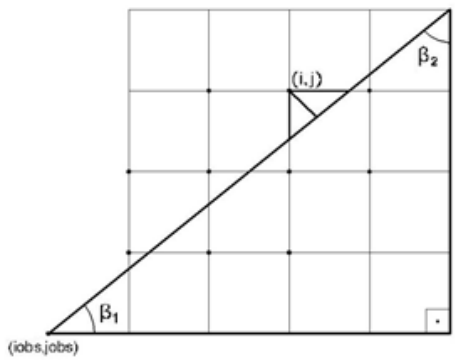

Fig. 3 Reference angles of triangle

where i, j is the cartesian coordinates of the closest point to the obstacle, and iobs is the starting point of the obstacle on the x-axis.

(c) There are 3 discrete directions that encounter obstacle nodes. For velocity direction 8,1 and 4,

$$\Delta = b \times a / \sqrt{2} \qquad \text{i=8} \qquad (14)$$

$$\Delta = \frac{a \times (i - iobs)}{(j - 0.5 - a)} \qquad \text{i=1} \qquad (15)$$

$$\Delta = a \qquad \text{i=4} \qquad (16)$$

According to values, modify the fluid particle's bounced distribution function with interpolation equations.

4. Parametrization for LBM

In general the dynamic behavior of a fluid can be expressed through the Reynolds number. It provides an estimation of the importance of the non-viscous and the viscous forces. Furthermore all simulations with the same Reynolds number have a similar dynamical behavior. The higher the Reynolds number, the more turbulent the flow is. The Reynolds number is determined by the inflow velocity, the diameter of the largest obstacle and the kinematic viscosity. These are physical parameters, but for the LBM algorithm only dimensionless quantities are used. The calculations of dimensionless lattice quantities are shown below with a superscript on real values:

$$\text{kinematic viscosity } \nu \left[\frac{m^2}{s}\right] : \nu^* = \nu \frac{\delta t}{\delta x^2} \qquad (17)$$

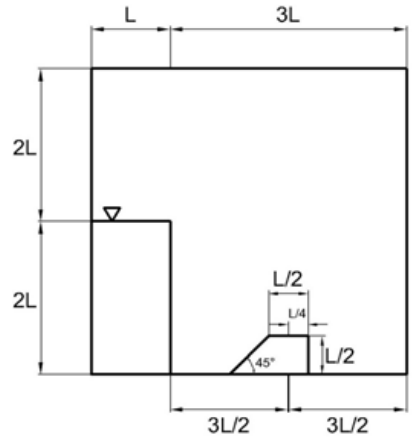

Fig. 4 Computational domain with trapezoidal obstacle

$$\text{gravity } g\left[\frac{m}{s^2}\right] \qquad : g^* = g \frac{\delta t^2}{\delta x} \qquad (18)$$

The relaxation time τ can be calculated via following way:

$$\tau = \frac{6\nu^* + 1}{2} \qquad (19)$$

It should be noted that τ can get certain values for the accurate and stable results of LBM. The numerical simulation becomes unstable particularly when the τ values close to 0.5.

5. Application and Computational Domain Details

In this paper, dam breaking over an obstacle application has been taken into account. Computational domain size and obstacle position can be seen in the Fig. 4. The dimensions and position of obstacle are exactly same with respect to L referred in reference [6], but we have scaled our computational domain with the scale ratio of 1/80 due to the memory problem. After scaling the dimension, L value has become 0.001425 m. Computational resolution has been set up 3 different sizes. The table given below contains all the parameters calculated for each grid size.

In addition to the length scale, we had to match the time with experimental data for accurate results. In order to match the time scale, we had to find out non-dimensional values for time. We obtained non-dimensional value of time every 0.05 second, from 0 to 2 second as same as reference [6], via following equation:

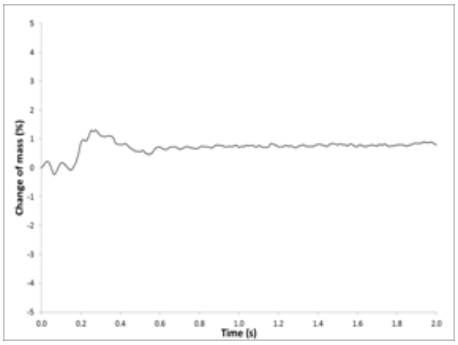

Fig. 5 The percentage of total mass change

$$t^* = t\sqrt{\frac{g}{L}} \tag{20}$$

where t* is non-dimensional time.

After obtaining non-dimensional values, we calculated our t values from same equation with the scaled L values. In other words, computational time was adapted to the experiment duration.

6. Comparative Results

Before showing the comparative results, mass conservation law has to be carefully investigated in order to simulate free surface flow. According to the equation 21, mass variation was checked during the whole computational duration.

$$\delta m = \frac{m_{init} - m_{comp}}{m_{init}} \times 100 \tag{21}$$

where δm is the change of mass, m_{init} is the initial mass and m_{comp} is the initant mass calculated every time step.

Fig. 5 shows the percentage of the mass change with respect to the computational time based on equation 21 as well as LBM 2 simulation conditions listed in table 1.

Table 1 Parameters of simulations

	LBM 1	LBM 2	LBM 3
Grid size	600*600	400*400	200*200
Non-dim. gravity	0.0007	0.0011	0.002
Viscosity (m2/s)	1.00E-06	1.00E-06	1.00E-06
Time step (s)	9.5E-06	1.43E-05	2.85E-05
Relaxation time	0.82	0.71	0.61

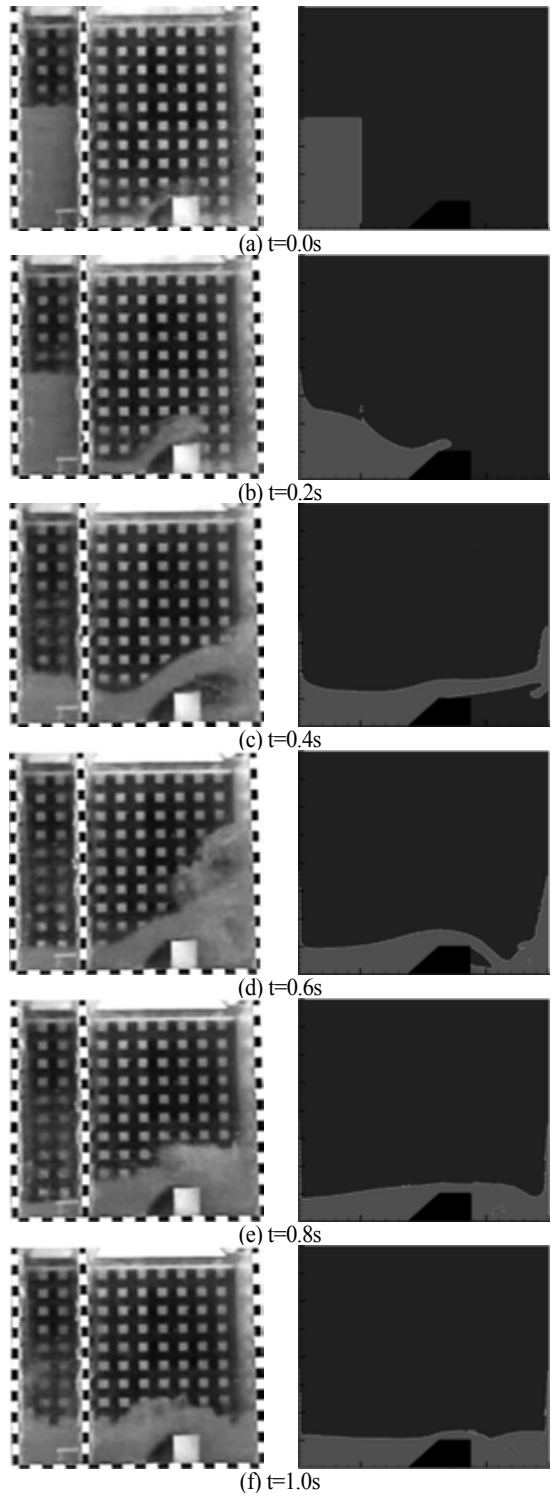

(a) t=0.0s (b) t=0.2s (c) t=0.4s (d) t=0.6s (e) t=0.8s (f) t=1.0s

Fig. 6 Free surface pattern comparision between experiment (left) and LBM 1 (right), from 0.0s (a) to 1.0s(f)

At the beginning of the simulation, we can see there are some fluctuations. However, it converges to the initial value by time. The percentage of mass change fluctuated between 1.4% and 0.3%, and it converges to 0.75%.

Following to the conservation of mass, we took the experimental results from reference [6] and compared them with the LBM results. Fig. 6 shows free surface motion comparison at every 0.2s based on LBM 2. From the Fig. 6(a) representing initial condition, LBM and experiment results are in good agreement. Due to the slope of trapezoidal obstacle, fluid flow reaches the similar maximum height on the right wall both in experiment and numerical result.

The dimensionless height of the free surface is shown by Fig. 7-9 during 2 second, including a numerical simulation reported by reference [6], LBM, and experimental data. Since we consider dam gate suddenly removed in LBM simulation, numerical simulation 1 data[6] is taken into account. Fig. 7 illustrates the evolution of dimensionless height at the left wall of the computational domain, whereas Fig. 8 and Fig. 9 illustrate at middle section of the obstacle and at the right wall of the computational domain, respectively. The computed results of LBM at left wall and right wall are overlapped with the experiment results. Small differences can be seen particularly in left wall free surface evolution, due to the gravitational force and the relaxation number effects. It should be noted that estimating fluid height at mid-point of obstacle needs new approach for both numerical study.

Fig. 7 and 9 also claims that increasing resolution results in more accurate results in terms of time. It can easily be seen that the first LBM simulation has more consistent results than the others. In Fig. 9, LBM 1 simulation has predicted the evolution of free surface nearly perfect by 1.4 second.

From the comparative results, the performance of LBM has been evaluated. LBM can capture the free surface movement as similar as experiment results. The turbulence modelling might be taken into account, especially in order to capture splashing effect on the right wall. Generally in the case of right wall where is the most important part of the domain, the height of the fluid changing by time is well overlapped with experiment. Furthermore, the height of mid-section of obstacle can be achieved coherently by modeling a finite speed of gate opening[6].

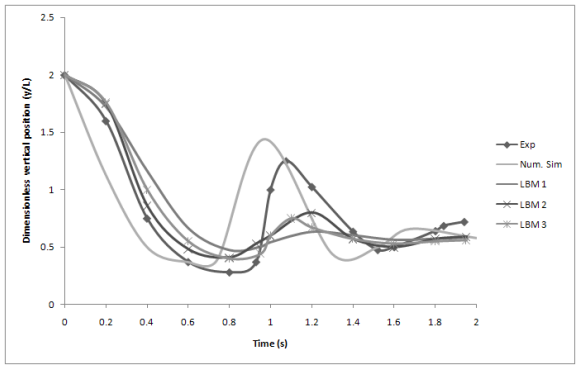

Fig. 7 Instant free surface evolution of vertical position at the left wall

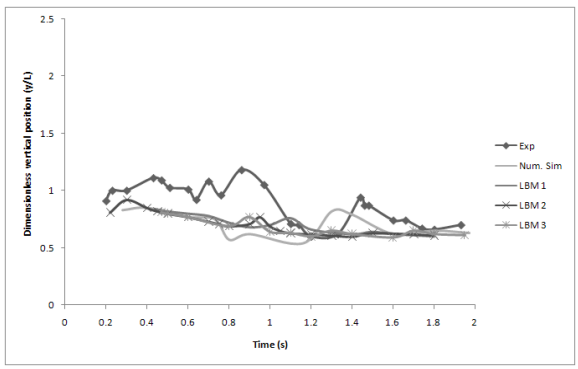

Fig. 8 Instant free surface evolution of vertical position at the mid-point of obstacle

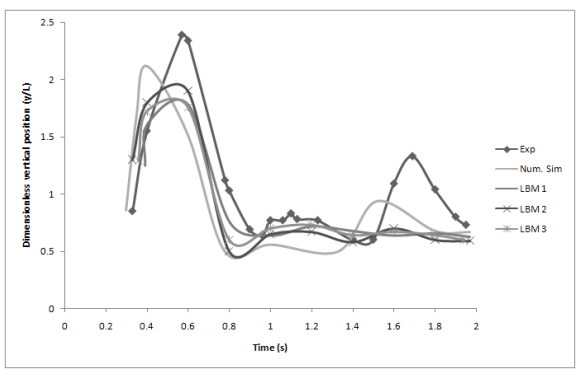

Fig. 9 Instant free surface evolution of vertical position at the right wall

7. Conclusion

Lattice Boltzmann Method is applicable for the simulation of the free surface flow over solid obstacle. In this paper, we have proposed an algorithm for inclined

wall. This algorithm can be used for different angles of slope. It is clear that geometrical rules should be considered for the derivation process of values. The algorithm can be easily adapted inverse shape of obstacle. To do that, local discrete velocity vectors should be modified with respect to the obstacle position. Moreover, computational resolution has to be considered while calculating values.

To sum up, there are two main outcomes from this study. Firstly, the generalized algorithm for inclined boundaries can be used to impose inclined obstacles for LBM. Secondly, the free surface pattern is evaluated by LBM coherently. Finally, grid dependency has not changed the precision in terms of fluid height prediction.

Acknowledgements

'This work was supported by the Research Fund of University of Ulsan.

References

[1] 1988, McNamara, G. R. and Zanetti, G., "Use of the Boltzmann Equation to Simulate Lattice-Gas Automata," *Physical Review Letters*, 61(20), pp.2332-2335.

[2] 2008, Mazzeo, M. D. and Coveney, P.V., "A High Per- formance Parallel Lattice-Boltzmann Code for Large Scale Fluid Flow in Complex Geometries," *Compute Physics Communications*, 178, pp.894-914.

[3] 1995, Inamuro, T., Yoshino, M. and Ogino, F., "A Non-slip Boundary Condition for Lattice Boltzmann Simulations," *Physics of Fluids*, 7, 2928-2930.

[4] 2001, Bouzidi, M., Firdaouss, M. and Lallemand, P., "Momentum Transfer of a Boltzmann-Lattice Fluid with Boundaries," *Physics of Fluids*, 13(11), pp.3452-3459.

[5] 1997, Filippova, O. and Hanel, D., "Lattice-Boltzmann Simulation of Gas Particle Flow in Filters," *Computers & Fluids*, 26(7), pp.697-712.

[6] 2009, Cruchaga, M.A., Celentano, D.J. and Tezduyar, T.E., "Computational Modeling of the Collapse of a Liquid Column Over an Obstacle and Experimental Validation," *Journal of Applied Mechanics*, 76, pp.021202-1-021202-5.

[7] 1954, Bhatnagar, P.L., Gross, E.P. and Krook, M., "A Model for Collision Processes in Gases. I. Small Amplitude Processes in Charged and Neutral One-Component Systems," *Physical Review*, 94(3), pp.511-525.

[8] 1997, He, X. and Luo, L.S., "A Priori Derivation of the Lattice Boltzmann Equation," *Physical Review E*, 55(6), pp.R6333-R6336.

[9] 1997, He, X. and Luo, L.S., "Lattice Boltzmann Model for the Incompressible Navier-Stokes Equation," *Journal of Statistical Physics*, 88, pp.927-944.

[10] 1994, Ladd, A.J.C., "Numerical Simulation of Particular Suspensions via a Discretized Boltzmann Equation Part 2," *Numerical Results. J. Fluid Mechanics*, 271, pp.311-339.

[11] 1993, Ziegler, D.P., "Boundary Conditions for Lattice Boltzmann Simulations," *Journal of Statistical Physics*, 71(5/6), pp.1171-1177.

[12] 2007, Thürey, N., "Physically based Animation of Free Surface Flows with the Lattice Boltzmann Method," *PhD thesis*.